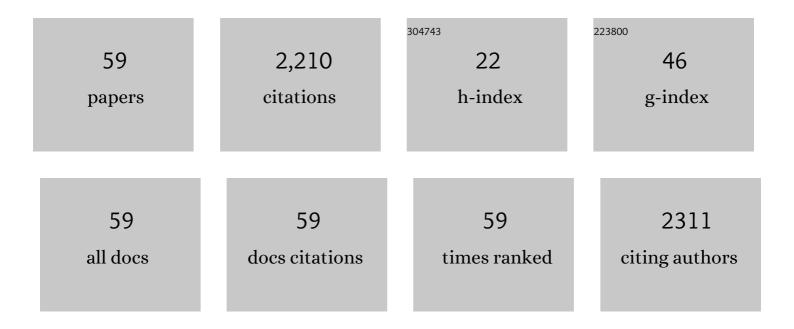
Takayuki Iwasaki

List of Publications by Year in descending order

Source: https://exaly.com/author-pdf/631486/publications.pdf Version: 2024-02-01



#	Article	IF	CITATIONS
1	Germanium-Vacancy Single Color Centers in Diamond. Scientific Reports, 2015, 5, 12882.	3.3	251
2	Tin-Vacancy Quantum Emitters in Diamond. Physical Review Letters, 2017, 119, 253601.	7.8	204
3	Well-posedness of feedback systems: insights into exact robustness analysis and approximate computations. IEEE Transactions on Automatic Control, 1998, 43, 619-630.	5.7	196
4	Al 2 O 3 / GeO x / Ge gate stacks with low interface trap density fabricated by electron cyclotron resonance plasma postoxidation. Applied Physics Letters, 2011, 98, .	3.3	143
5	Long-Range Ordered Single-Crystal Graphene on High-Quality Heteroepitaxial Ni Thin Films Grown on MgO(111). Nano Letters, 2011, 11, 79-84.	9.1	141
6	The dual iteration for fixed-order control. IEEE Transactions on Automatic Control, 1999, 44, 783-788.	5.7	124
7	Direct Nanoscale Sensing of the Internal Electric Field in Operating Semiconductor Devices Using Single Electron Spins. ACS Nano, 2017, 11, 1238-1245.	14.6	82
8	600 V Diamond Junction Field-Effect Transistors Operated at 200\$^{circ}{m C}\$. IEEE Electron Device Letters, 2014, 35, 241-243.	3.9	74
9	Magnetometer with nitrogen-vacancy center in a bulk diamond for detecting magnetic nanoparticles in biomedical applications. Scientific Reports, 2020, 10, 2483.	3.3	66
10	Spectroscopic investigations of negatively charged tin-vacancy centres in diamond. New Journal of Physics, 2020, 22, 013048.	2.9	62
11	Diamond Junction Field-Effect Transistors with Selectively Grown n\$^{+}\$-Side Gates. Applied Physics Express, 2012, 5, 091301.	2.4	61
12	Formation of perfectly aligned nitrogen-vacancy-center ensembles in chemical-vapor-deposition-grown diamond (111). Applied Physics Express, 2017, 10, 045501.	2.4	49
13	Effect of radical fluorination on mono- and bi-layer graphene in Ar/F2 plasma. Applied Physics Letters, 2012, 101, .	3.3	45
14	Perfectly aligned shallow ensemble nitrogen-vacancy centers in (111) diamond. Applied Physics Letters, 2017, 111, .	3.3	45
15	Effect of Si, Ge and Sn dopant elements on structure and photoluminescence of nano- and microdiamonds synthesized from organic compounds. Diamond and Related Materials, 2019, 93, 75-83.	3.9	38
16	A quantum thermometric sensing and analysis system using fluorescent nanodiamonds for the evaluation of living stem cell functions according to intracellular temperature. Nanoscale Advances, 2020, 2, 1859-1868.	4.6	37
17	Normally-Off Diamond Junction Field-Effect Transistors With Submicrometer Channel. IEEE Electron Device Letters, 2016, 37, 209-211.	3.9	36
18	Electrical properties of lateral p–n junction diodes fabricated by selective growth of n ⁺ diamond. Physica Status Solidi (A) Applications and Materials Science, 2012, 209, 1761-1764.	1.8	32

ΤΑΚΑΥUKI IWASAKI

#	Article	IF	CITATIONS
19	Quantifying selective alignment of ensemble nitrogen-vacancy centers in (111) diamond. Applied Physics Letters, 2015, 107, .	3.3	31
20	High-Temperature Bipolar-Mode Operation of Normally-Off Diamond JFET. IEEE Journal of the Electron Devices Society, 2017, 5, 95-99.	2.1	27
21	Simultaneous thermometry and magnetometry using a fiber-coupled quantum diamond sensor. Applied Physics Letters, 2021, 118, .	3.3	26
22	Extending coherence time of macro-scale diamond magnetometer by dynamical decoupling with coplanar waveguide resonator. Review of Scientific Instruments, 2018, 89, 125007.	1.3	25
23	Integrated system design by separation. , 0, , .		23
24	Asymmetric transport property of fluorinated graphene. Applied Physics Letters, 2013, 103, 143106.	3.3	21
25	Improved visible light driven photoelectrochemical properties of 3C-SiC semiconductor with Pt nanoparticles for hydrogen generation. Applied Physics Letters, 2013, 103, .	3.3	20
26	Formation and structural analysis of twisted bilayer graphene on Ni(111) thin films. Surface Science, 2014, 625, 44-49.	1.9	18
27	Charge state modulation of nitrogen vacancy centers in diamond by applying a forward voltage across a p–i–n junction. Diamond and Related Materials, 2016, 63, 192-196.	3.9	18
28	Simultaneous wide-field imaging of phase and magnitude of AC magnetic signal using diamond quantum magnetometry. Scientific Reports, 2020, 10, 11611.	3.3	18
29	Heteroepitaxial growth of diamond films on 3C-SiC/Si substrates with utilization of antenna-edge microwave plasma CVD for nucleation. Japanese Journal of Applied Physics, 2015, 54, 04DH13.	1.5	17
30	Highly oriented diamond (111) films synthesized by pulse bias-enhanced nucleation and epitaxial grain selection on a 3C-SiC/Si (111) substrate. Applied Physics Letters, 2017, 110, .	3.3	17
31	Vector Electrometry in a Wide-Gap-Semiconductor Device Using a Spin-Ensemble Quantum Sensor. Physical Review Applied, 2020, 14, .	3.8	17
32	Coherence of a charge stabilised tin-vacancy spin in diamond. Npj Quantum Information, 2022, 8, .	6.7	16
33	LPV system analysis with quadratic separator. , 0, , .		15
34	When is (D,G)-scaling both necessary and sufficient. IEEE Transactions on Automatic Control, 2000, 45, 1755-1759.	5.7	15
35	Vector magnetometry using perfectly aligned nitrogen-vacancy center ensemble in diamond. Applied Physics Letters, 2021, 118, .	3.3	14
36	Low-Temperature Spectroscopic Investigation of Lead-Vacancy Centers in Diamond Fabricated by High-Pressure and High-Temperature Treatment. ACS Photonics, 2021, 8, 2947-2954.	6.6	14

ΤΑΚΑΥUKI IWASAKI

#	Article	IF	CITATIONS
37	Wide-field diamond magnetometry with millihertz frequency resolution and nanotesla sensitivity. AIP Advances, 2018, 8, .	1.3	13
38	Thermal Stability of Perfectly Aligned Nitrogenâ€Vacancy Centers for High Sensitive Magnetometers. Physica Status Solidi (A) Applications and Materials Science, 2018, 215, 1800342.	1.8	13
39	In situ bias current monitoring of nucleation for epitaxial diamonds on 3C-SiC/Si substrates. Diamond and Related Materials, 2018, 88, 158-162.	3.9	13
40	Preferentially aligned nitrogen-vacancy centers in heteroepitaxial (111) diamonds on Si substrates via 3C-SiC intermediate layers. Applied Physics Express, 2018, 11, 045501.	2.4	12
41	Thermometric quantum sensor using excited state of silicon vacancy centers in 4H-SiC devices. Applied Physics Letters, 2021, 118, .	3.3	12
42	Characterization of Schottky Barrier Diodes on Heteroepitaxial Diamond on 3C-SiC/Si Substrates. IEEE Transactions on Electron Devices, 2020, 67, 212-216.	3.0	11
43	High growth rate synthesis of diamond film containing perfectly aligned nitrogen-vacancy centers by high-power density plasma CVD. Diamond and Related Materials, 2022, 123, 108840.	3.9	11
44	Charge-state control of ensemble of nitrogen vacancy centers by n–i–n diamond junctions. Applied Physics Express, 2018, 11, 033004.	2.4	10
45	Influence of high-power density plasma on heteroepitaxial diamond nucleation on 3C-SiC surface. Applied Physics Express, 2017, 10, 045502.	2.4	9
46	Photoelectrical detection of nitrogen-vacancy centers by utilizing diamond lateral p–i–n diodes. Applied Physics Letters, 2021, 118, .	3.3	9
47	Gradiometer Using Separated Diamond Quantum Magnetometers. Sensors, 2021, 21, 977.	3.8	8
48	LPV system analysis via quadratic separator for uncertain implicit systems. , 0, , .		7
49	Polarizationâ€controlled dressedâ€photon–phonon etching of patterned diamond structures. Physica Status Solidi (A) Applications and Materials Science, 2014, 211, 2339-2342.	1.8	7
50	Fabrication of diamond lateral p–n junction diodes on (111) substrates. Physica Status Solidi (A) Applications and Materials Science, 2015, 212, 2548-2552.	1.8	7
51	Labelâ€Free Phase Change Detection of Lipid Bilayers Using Nanoscale Diamond Magnetometry. Advanced Quantum Technologies, 2021, 4, 2000106.	3.9	7
52	Observation of Interface Defects in Diamond Lateral p-n-Junction Diodes and Their Effect on Reverse Leakage Current. IEEE Transactions on Electron Devices, 2017, 64, 3298-3302.	3.0	6
53	Color centers based on heavy group-IV elements. Semiconductors and Semimetals, 2020, 103, 237-256.	0.7	5
54	Magnetic Field Generation System of the Magnetic Probe With Diamond Quantum Sensor and Ferromagnetic Materials for the Detection of Sentinel Lymph Nodes With Magnetic Nanoparticles. IEEE Transactions on Magnetics, 2021, 57, 1-5.	2.1	5

ΤΑΚΑΥUKI IWASAKI

#	Article	IF	CITATIONS
55	Fluorinated Graphene FETs Controlled by Ionic Liquid Gate. Journal of Display Technology, 2014, 10, 962-965.	1.2	2
56	Diamond electronics. , 2016, , .		2
57	Dynamical function design from a control perspective. , 0, , .		1
58	Determination of Current Leakage Sites in Diamond p–n Junction. Physica Status Solidi (A) Applications and Materials Science, 2019, 216, 1900243.	1.8	1
59	Device engineering for diamond quantum sensors. , 2019, , .		1